Optical Materials 32 (2010) 510–514

Contents lists available at ScienceDirect

Optical Materials

journal homepage: www.elsevier.com/locate/optmat

Optical and structural properties of silver nanoparticles in glass matrix formed by thermal annealing of field assisted film dissolution

J. Sancho-Parramon [a,*], V. Janicki [a], P. Dubček [a], M. Karlušić [a], D. Gracin [a], M. Jakšić [a], S. Bernstorff [b], D. Meljanac [a], K. Juraić [a]

[a] Rudjer Boskovic Institute, Bijenicka cesta 54, 10000 Zagreb, Croatia
[b] Sincrotrone Trieste, in AREA Science Park, 34012 Basovizza/Trieste, Italy

ARTICLE INFO

Article history:
Received 10 August 2009
Received in revised form 6 November 2009
Accepted 14 November 2009
Available online 16 December 2009

Keywords:
Metal nanoparticles
Electric field assisted dissolution
Surface plasmon resonance

ABSTRACT

A two-step procedure for the formation of silver nanoparticles embedded in a glass matrix is studied. The procedure consists of: (i) the inclusion of silver ions in the glass matrix by electric field assisted dissolution of Ag film deposited on the glass and (ii) the aggregation of silver by thermal annealing. The optical properties of the sample, dominated by the surface plasmon resonance of metal nanoparticles in the visible spectral range, are studied by optical spectroscopy. The structural characterization is carried out by grazing-incidence small-angle X-ray scattering measurements performed at the Synchrotron Elettra (Italy) and silver depth profiles are determined using Rutherford backscattering. The results suggest that the depth profile of Ag might be tailored by modification of the parameters of metal film dissolution (electric field and temperature). Variation of thermal annealing parameters (temperature and time) allows control of the nanoparticles size. Thus, the surface plasmon absorption intensity and line shape are changed, enabling tuning of the optical properties of the sample.

1. Introduction

Glasses containing metal nanoparticles are focus of intense research because of their unique optical properties. Due to the surface plasmon resonance (SPR) of metal free electrons, absorption and scattering by nanoparticles and strong field enhancement take place. SPR properties strongly depend on the size and shape distribution of nanoparticles as well as on the interparticle interaction [1]. Consequently, a wide variety of linear and non-linear applications of dielectrics with embedded nanoparticles have been designed, such as selective absorbers [2], polarizers [3], diffraction gratings [4], optical switches [5] or solar cells [6].

2Several methods for the formation of metal nanoparticles in glass matrix have been developed, like low energy ion–beam mixing [7], sol–gel [8], direct metal-ion implantation [9], light-ion irradiation in ion-exchanged glasses [10], annealing in hydrogen atmosphere of ion-exchanged glasses [11] and single-step ion exchange [12,10]. Most of these methods consist of a two-step process: (i) the inclusion of metal ions into the glass matrix and (ii) the formation of clusters upon post-inclusion treatment [13]. The possibility of ion inclusion in glass matrix by the electric field assisted dissolution of a film at moderately elevated temperatures has been recently investigated for transition metals [14]. Formation of metal aggregates upon thermal annealing of glasses in which electric field assisted dissolution of nanoparticles was performed has been also reported [6]. This approach is technologically attractive due to its simplicity and inexpensive technical requirements.

In the present work we study the formation of silver nanoparticles in a glass substrate by the electric field assisted dissolution of a film deposited on the glass surface and subsequent thermal annealing in air. This approach is of high technological interest as it combines well-established thin film deposition techniques and inexpensive film dissolution and thermal treatments. The optical, compositional and structural properties of glasses after the film dissolution and after thermal annealing are investigated using optical spectroscopy, Rutherford backscattering (RBS) and grazing-incidence small-angle X-ray scattering (GISAXS). The results suggest the possibility to tailor the optical properties of the samples through modifications of nanoparticle size and depth distribution that can be achieved by controlling the treatment parameters of film dissolution (temperature and applied electric field) and post-inclusion annealing (temperature and time).

2. Experimental

2.1. Formation of nanoparticles

Borosilicate (BK7) glass substrates 1 mm-thick were coated with a 100 nm-thick Ag film by electron beam evaporation in a

* Corresponding author. Tel.: +385 1 4571 247; fax: +385 1 4680 104.
E-mail address: jsancho@irb.hr (J. Sancho-Parramon).

0925-3467/$ - see front matter © 2009 Elsevier B.V. All rights reserved.
doi:10.1016/j.optmat.2009.11.004

Varian 3117 deposition chamber. Dissolution of the deposited film into the glass matrix was induced by simultaneous application of constant voltage (V_{EFAD}) and temperature (T_{EFAD}) in a similar way to our previous work on electric field assisted dissolution of metal islands [15]. The electric field was applied perpendicularly to the sample surface with the cathode facing the film. Glass substrates coated with 700 nm-thick Cr thin film were used as electrodes. When using mechanically polished metal plates as electrodes, the electric field dissolution was inhomogeneous due to the non-uniform contact between sample and electrode, as reported in [16]. Cr thin films, however, presented a very flat surface and the contact between electrode and Ag layer was smoother, resulting in homogeneous field dissolution through the sample surface. The electric field was applied during two hours. In all the cases, after this time the Ag layer was completely dissolved, i.e., no Ag residual film remained on the glass surface. After the film dissolution, samples were annealed for different times (t) at different temperatures (T_{ANNEAL}) in order to induce Ag clustering and nanoparticle formation. Annealing temperatures were limited up to 600 °C to avoid glass softening.

2.2. Characterization techniques

Optical spectroscopy was used to characterize the glasses after the film dissolution and to detect the SPR of nanoparticles in the annealed samples. Transmittance measurements at normal incidence were carried out in a Perkin Elmer Lambda 25 spectrophotometer in the spectral range between 300 and 1100 nm.

Silver depth profiles were determined by Rutherford backscattering measurements using 1.6 MeV proton beam from the 1.0 MV Tandetron accelerator at the Ruđer Bošković Institute in Zagreb (Croatia) [17]. Spectra were collected using a surface barrier detector with 15 keV energy resolution positioned at 165° relative to the beam direction. The analysis of the spectra was performed with the SIMNRA code [18] using non-Rutherford cross sections data base. Silver concentration is typically detected with an accuracy of 0.1–0.5% of its absolute value.

GISAXS measurements enable the detection of objects (particles) of nanometric dimensions by analysis of scattering patterns of X-ray radiation incising the sample at grazing angles. The quantitative analysis of the data allows determining morphological parameters, such as the object dimensions. In opposition to other morphological characterization methods, such as transmission electron microscopy, the GISAXS technique is non-destructive and gives information of relatively large area (beam spot up to few mm) thus providing statistically-averaged data of many particles. The GISAXS measurements were performed at the Austrian SAXS beam line [19] at the Synchrotron ELETTRA in Trieste (Italy), using 8 keV X-ray photon energy (λ = 0.154 nm). The GISAXS intensity curves are obtained from the scattering pattern recorded by a two-dimensional charge-coupled device (CCD) sensitive detector with image size of 1024 × 1024 pixels. The detector to sample distance was L = 2.0 m. A motorized Al beam stop was positioned perpendicularly to the sample surface to reduce the transmitted and specularly reflected beams. The samples were mounted on a stepper-motor-controlled tilting stage with a step resolution of 0.001° and measured at the chosen grazing angles.

3. Results

3.1. Optical spectroscopy

The extinction spectrum (negative logarithm of transmittance) of glass after film dissolution with parameters T_{EFAD} = 300 °C and V_{EFAD} = 1.6 kV is shown in Fig. 1. The sample is transparent in the whole spectral range of measurements confirming the dissolution of the Ag film. In addition, small oscillations in the optical spectra can be observed (solid black line in inset of Fig. 1), that can be associated to weak interferential fringes. Since the amplitude of these fringes is very small, they suggest the presence of a surface layer with slightly different refractive index than the rest of glass. After film dissolution, the sample was cut into several pieces that were annealed for 2 h at different temperatures (T_{ANNEAL}), whose spectra are also shown in Fig. 1. The samples annealed at 560 °C and 600 °C show an absorption peak in the region between 410 and 460 nm that can be identified to the SPR of silver nanoparticles. This peak follows a blue-shift as the annealing temperature increases, approaching to 410 nm for the sample annealed at 560 °C, which corresponds to the SPR of bulk silver nanoparticles in glass matrix. The absorption peak is very weak for the sample annealed at 460 °C and increases for the samples annealed at higher temperatures, indicating an increase of the total volume fraction of particles. Moreover, the SPR peak becomes narrower as T_{ANNEAL} increases. An estimation of the particle size can be done assuming that (i) the extinction spectra can be described with the Mie theory and (ii) the dielectric function of silver follows the Drude model including a broadening term that is size-dependent due to the shortening of electron free path as the particle size reduces [1]. Under such assumptions, the particle size (d) can be estimated as $d = V_F/\Delta\omega$, where V_F is the Fermi velocity for free electrons in Ag and $\Delta\omega$ is the full width at half maximum of the SPR absorption peak. For the spectra shown in Fig. 1 d equals 0.99 nm, 2.45 nm and 5.10 nm for the samples annealed at T_{ANNEAL} = 460 °C, 560 °C and 600 °C, respectively. In addition to the appearance of the SPR peak, the interference fringes observed in the glass after film dissolution vanish as T_{ANNEAL} increases.

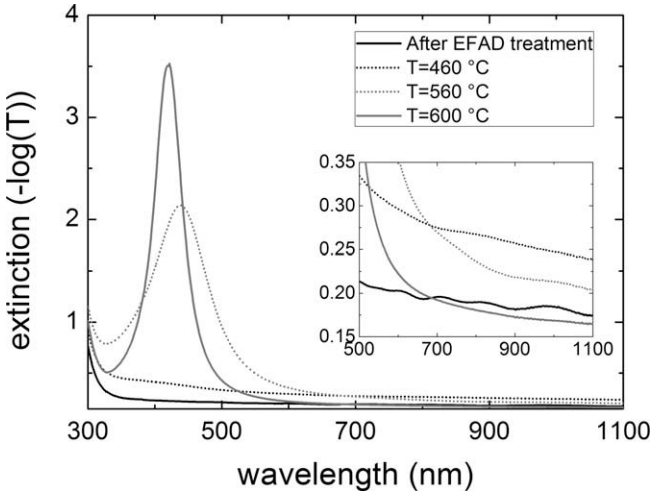

Fig. 1. Extinction spectra of samples treated at V_{EFAD} = 1.6 kV and T_{EFAD} = 300 °C after film dissolution (solid line) and after annealing for 2 h at different T_{ANNEAL}: 460 °C (dashed line), 560 °C (dotted line), 600 °C (dashed-dotted line).

3.2. Rutherford backscattering

RBS spectra for samples treated at T_{EFAD} = 300 °C and V_{EFAD} = 1.6 kV and V_{EFAD} = 0.4 kV are shown in Fig. 2a and b, respectively. Spectra for the sample after the film dissolution and after different thermal annealing treatments are shown, indicating the presence of different elements in the glass. The corresponding Ag depth profiles retrieved from the experimental spectra are shown in Fig. 3. For the samples after film dissolution, Ag is basically concentrated in a region of up to few microns from the glass surface. This region is located very close to the surface for the case of the sample trea-

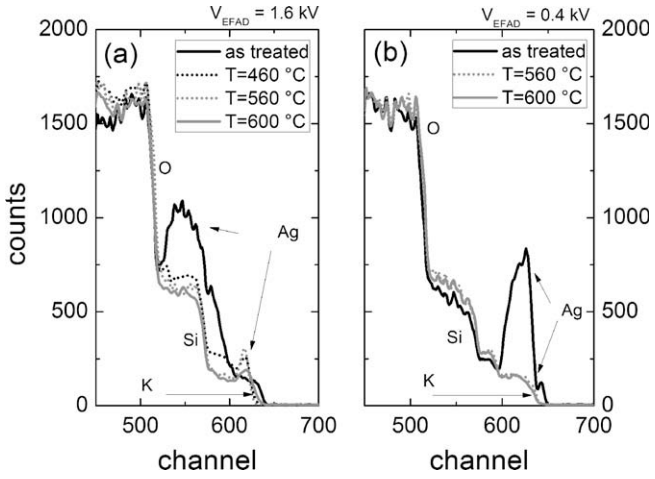

Fig. 2. RBS spectra for the samples treated at V_{EFAD} = 1.6 kV and T_{EFAD} = 300 °C (a) and V_{EFAD} = 0.4 kV and T_{EFAD} = 300 °C (b) after film dissolution and annealed for 2 h at different T_{ANNEAL}. The *X*-axis (channel) is related to the energy of the backscattered protons.

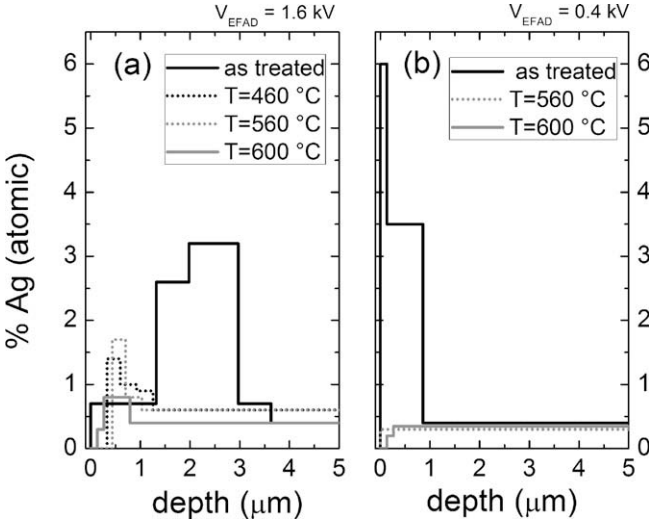

Fig. 3. Ag depth profiles extracted from RBS measurements on the samples from Fig. 2.

ted at V_{EFAD} = 0.4 kV and at 2–3 microns in-depth for the sample treated at V_{EFAD} = 1.6 kV. The depth profiles for the annealed samples indicate a diffusion of Ag through the glass. For the case of the sample treated at V_{EFAD} = 1.6 kV, as T_{ANNEAL} is increased, besides the broadening of the peak in the Ag profile, the maximum of Ag concentration moves closer to the surface.

3.3. GISAXS

GISAXS scattering patterns for samples in which the film dissolution parameters were T_{EFAD} = 300 °C and V_{EFAD} = 0.8 kV, and annealed at different temperatures and times are shown in Fig. 4. The patterns show the scattered intensity as a function of the scattering wave vector **q** in the *z* (perpendicular to the sample surface) and *y* (parallel to the sample surface) directions. The module of **q** is $4\pi \sin\theta/\lambda$, where 2θ is the X-ray scattering angle. Except for the sample annealed at T_{ANNEAL} = 460 °C for two hours, the scattering patterns indicate the presence of nano-objects with an electronic density different than the glass matrix, that can be identified as silver nanoparticles. Assuming an ellipsoidal shape, the particle horizontal and vertical dimensions (i. e., in the directions parallel and perpendicular to the glass surface) were estimated using the Guinier approximation in the analysis of the 1D intensity distributions in the two characteristic directions parallel and perpendicular to the surface [20]. Basically, the particle size is estimated from the slope of a logarithmic plot of the scattered intensity versus the square of the wave vector, that is expected to show a linear dependence for small wave vectors. Table 1 summarizes the results for the samples shown in Fig. 4, indicating that the particles have a near-spherical shape and that higher T_{ANNEAL} or longer annealing times induce an increase of the particles size. The particle size estimation by GISAXS is in good agreement with the values obtained from optical spectroscopy.

4. Discussion

The inclusion of Ag in glass by electric field assisted film dissolution is evidenced by RBS, indicating that silver is mainly distributed in a region beneath the glass surface typically 1–2 microns thick. Due to the presence of Ag, such region will present a higher refractive index than the rest of the glass matrix, as reported in [21], what can explain the interferential fringes of very small amplitude observed by optical spectroscopy. Indeed, the modification of the refractive index of glass by metal ion implantation or ion exchange has been used for the fabrication of waveguides [21]. The phenomenon of ion inclusion in glass matrix by film dissolution is usually assumed to initiate by the temperature-induced oxidization of the metal film. In this way the oxide layer at the interface can supply Ag^+ for ion diffusion upon application of electric field [22]. In addition alkali ion migration of native ions inside the glass (basically Na^+) is faster than the diffusion of metal, generating a space-charge distribution inside the glass and modifying the diffusion of metal ions [14]. Thus, the distribution of metal ions inside the glass depends in a complex way on the physical and chemical phenomena that take place at the metal–glass interface and in the glass. As pointed out in [23], a complete modeling of the ion diffusion process is still lacking. In any case, in the studied samples we showed that by varying the applied electric field, the depth distribution of Ag can be modified, with a concentration maximum at the surface (V_{EFAD} = 0.4 kV), as usual in field assisted film dissolution [24], or at certain depth within the glass (V_{EFAD} = 1.6 kV), that has been previously associated to a lack of local charge neutrality due to structural network modifications upon the formation of a strongly depleted region [14]. Such region can be formed as the applied electric field is higher. In addition, for all applied electric fields the Ag layer was completely dissolved. As the film dissolution is expected to take place faster the higher the electric field, for the sample treated with V_{EFAD} = 1.6 kV the electric field was applied for a longer period to the glass containing all Ag ions without further supply from Ag layer, in respect to the sample treated with V_{EFAD} = 0.4 kV. This difference could enhance the lack of local charge neutrality and give place to Ag concentration maximum at some glass depth. A deeper analysis of the dependence of the metal depth profile with V_{EFAD} and T_{EFAD} will be subject of future research. In this sense, RBS measurements using heavier ions could permit to obtain a more detailed Ag depth profile that enables modeling of the ion-diffusion process.

The Ag profile broadens and becomes nearly homogeneous throughout the glass (up to the depth limit detectable by RBS) upon annealing. Such broadening corresponds to the thermal diffusion of the Ag concentration and has been previously reported for Ag in glass matrix produced by ion-exchange process [25,26]. The broadening of Ag concentration reduces the increase of refractive index in the Ag-containing region, what explains the vanishing of interference fringes upon increase of T_{ANNEAL}. For the sample trea-

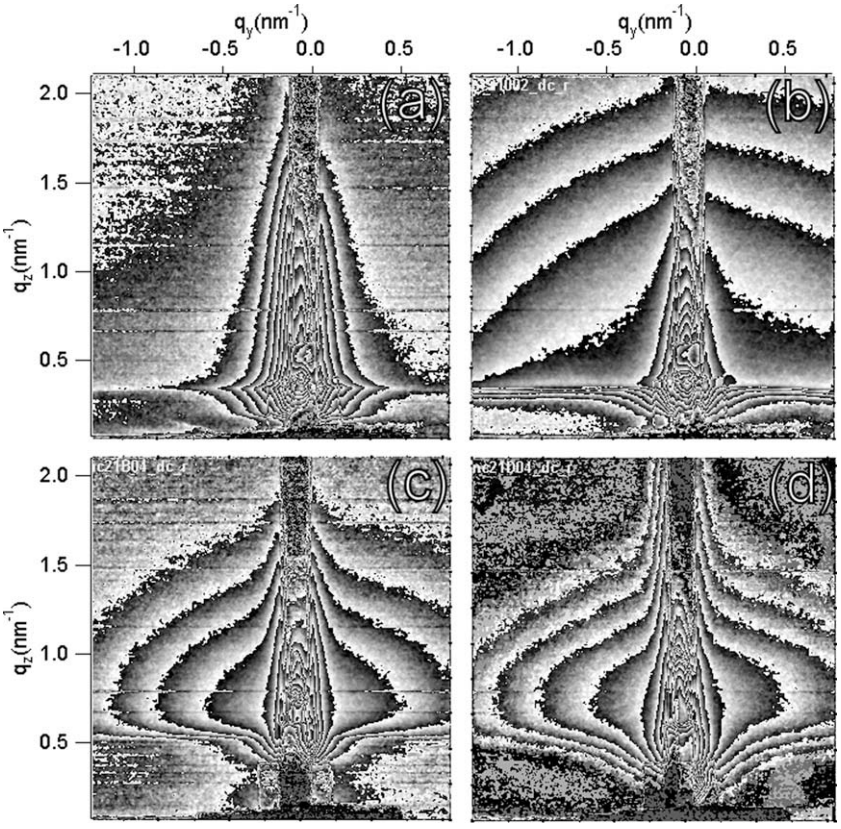

Fig. 4. GISAXS diffraction patterns for samples treated at V_{EFAD} = 0.8 kV and T_{EFAD} = 300 °C and annealed for: 2 h at 460 °C (a), 6 h at 460 °C (b), 2 h at 560 °C (c) and 2 h at 600 °C (d).

Table 1
Particles size determined by GISAXS and optical spectroscopy (OS) for samples treated at V_{EFAD} = 0.8 kV and T_{EFAD} = 300 °C and annealed for: 2 h at 460 °C (a), 6 h at 460 °C (b), 2 h at 560 °C (c) and 2 h at 600 °C (d).

Sample	a	b	c	d
GISAXS vertical size (nm)	–	3.0	5.2	5.2
GISAXS horizontal size (nm)	–	3.2	4.2	4.9
OS size (nm)	–	2.9	4.2	4.6

ted at V_{EFAD} = 1.6 kV, besides the broadening of the profile, a shift of the Ag concentration peak towards the surface is detected. The diffusion of Ag concentration outwards has been observed in [27] and associated to a stress relaxation that arises from the size difference of Ag^+ and Na^+. From RBS spectra, however, it is not possible to detect the evolution of the Na concentration profile since the corresponding signal is masked by other elements.

High temperatures and long annealing times induce the formation and growth of silver nanoparticles, as evidenced by optical spectroscopy and GISAXS, in agreement with previous works [27,28]. The blue shift of the SPR with the annealing temperature can be associated to spill-out effects [29]: for very small particles (typically below 5 nm) the wave function of free electrons extends beyond the particle diameter, resulting in a reduction of the effective average electron density with respect to that of bulk metal. As a consequence, the SPR for very small particles is red-shifted from that of bulk metal, as observed experimentally. The formation of nanoparticles by annealing at normal atmosphere requires the reduction of Ag ions and their subsequent clustering [26]. In this sense, high annealing temperatures have to be supplied for particle formation compared to annealing at hydrogen atmosphere, where due to the presence of a reducing agent lower temperatures suffice [26]. Owing to the thermal diffusion of silver through the glass, the concentration of silver is low (~0.4% as shown by RBS), justifying that the optical properties of the glass containing particles can be well described by the Mie theory and interaction between particles can be neglected. Under these assumptions, size determination from SPR breadth is a good approximation [30]. The methods used for particle size determination (optical spectroscopy and GISAXS) give numerically precise sizes (with uncertainties in the order of few percent), but if the assumptions made on the corresponding approximations are not fulfilled, misleading results can be obtained. The good agreement between both methods suggests that these assumptions are realistic for the studied samples.

5. Conclusions

Silver nanoparticles of a few nanometers in size embedded in a glass matrix have been formed by electric field assisted dissolution of a silver film deposited on glass and subsequent thermal annealing. The Ag concentration profile within the glass matrix formed after film dissolution depends on the treatment parameters what suggests the possibility to control the Ag depth profile by modification of the applied electric field and treatment time. After thermal annealing the profile broadens and the distribution of Ag in the glass depth detectable by RBS is nearly homogeneous. Annealing also induces the formation of nanoparticles, whose size increases with the annealing temperature or time. Thus, since the SPR strongly depends on the nanoparticle size, the optical properties of the glass containing Ag particles can be tailored by the thermal annealing treatment. The location of Ag, however, can not be controlled, as thermal annealing induces Ag diffusion. The use of other methods to avoid temperature-induced metal diffusion, like ion irradiation, could allow the formation of nanoparticles with a

depth distribution similar to the one obtained upon film dissolution. Overall, the described approach is technologically attractive as combines well-known film deposition techniques and relatively simple post-deposition treatments. In this sense, this approach may take advantage of the widely developed thin film fabrication methods what could open up the possibility to vary other parameters of particles embedded in glass, such as the particle composition by the simultaneous co-deposition of different metals.

Acknowledgments

J.S.P. thanks the financial support of the Catalan Government through a "Beatriu de Pinós" postdoctoral grant.

References

[1] U. Kreibig, M. Vollmer, Optical Properties of Metal Clusters, Springer, Berlin, 1995.
[2] S. Kachan, O. Stenzel, A. Ponyavina, App. Phys. B: Lasers Opt. 84 (2006) 281.
[3] K. Baba, J. Katsu, M. Miyagi, Opt. Lett. 17 (1992) 622.
[4] P. Faccio, D.I. Trapani, E. Borsella, F. Gonella, P. Mazzoldi, A.M. Malvezzo, Europhys. Lett. 43 (1998) 213.
[5] G. Seifert, M. Kaempfe, K.-J. Berg, H. Graener, Appl. Phys. B 73 (2001) 355.
[6] F. Hallermann, C. Rockstuhl, S. Fahr, G. Seifert, S. Wackerow, H. Graener, G.V. Plessen, F. Lederer, Phys. Stat. Sol. (a) 205 (2008) 2844.
[7] P. Gangopadhyay, R. Kesavamoorthy, K.G.M. Nair, R. Dhandapani, J. Appl. Phys. 88 (2000) 4975.
[8] M. Epifani, C. Giannini, L. Tapfer, L. Vasanelli, J. Am. Ceram. Soc. 83 (2000) 2385.
[9] Z. Liu, H. Wang, H. Li, X. Wang, Appl. Phys. Lett. 72 (1998) 1823.
[10] M. Dubiel, R. Schnerider, H. Hofmeister, H.D. Schicke, J.C. Pivin, Eur. Phys. J. D 43 (2007) 291.
[11] G. de Marchi, F. Caccavale, F. Gonella, G. Mattei, P. Mazzoldi, G. Bataglin, A. Quaranta, Appl. Phys. A 63 (1996) 403.
[12] G. Medhi, P. Nandi, S. Mohan, G. Jose, Mater. Lett. 61 (2007) 2259.
[13] F. Gonella, Rev. Adv. Mater. Sci. 14 (2007) 134.
[14] F. Gonella, E. Cattaruzza, A. Quaranta, S. Ali, N. Argiolas, C. Sada, Solid State Ionics 177 (2006) 3151.
[15] J. Sancho-Parramon, V. Janicki, J. Arbiol, H. Zorc, F. Peiro, Appl. Phys. Lett. 92 (2008) 163108.
[16] O. Deparis, P.G. Kazansky, A. Podlipensky, A. Abdolvand, G. Seifert, H. Graener, Appl. Phys. Lett. 86 (2005) 261109.
[17] M. Jakšić, Nucl. Instr. and Meth. B 260 (2007) 114.
[18] M. Mayer, Nucl. Instr. and Meth. B 194 (2002) 177.
[19] H. Amenitsch, M. Rappolt, M. Kriechbaum, H. Mio, P. Laggner, S. Bernstorff, J. Synchrotron Radiat. 5 (1998) 506.
[20] A. Guinier, S.G. Fourne, Small angle scattering of X-rays, Wiley, New York, 1955.
[21] S. Honkanen, A. Tervonen, J. Appl. Phys. 63 (1988) 634.
[22] D. Kapila, J.L. Plawsky, Chem. Eng. Sci. 50 (1995) 2589.
[23] A. Quaranta, E. Cattaruzza, F. Gonella, Mater. Sci. Eng. B 149 (2008) 133.
[24] M. Abou el Leil, A.R. Cooper, J. Am. Ceram. Soc. 62 (1979) 390.
[25] K.J. Berg, P. Grau, D. Nowak-Wozny, M. Petzold, M. Suszynska, Mater. Chem. Phys. 40 (1995) 131.
[26] E. Borsella, E. Cattaruzza, G. De Marchi, F. Gonella, G. Mattei, P. Mazzoldi, A. Quaranta, G. Battaglin, R. Polloni, J. Non-Cryst. Solids 245 (1999) 122.
[27] P. Gangodpanhyay, P. Magudapathy, R. Kesavamoorthy, B.K. Panigrahi, K.G.M. Nair, P.V. Satyam, Chem. Phys. Lett. 388 (2004) 416.
[28] J.Ph. Blondeau, F. Catan, C. Andreazza-Vignolle, N. Sbai, Plasmonics 3 (2008) 65.
[29] J. Lermé, B. Palpant, B. Prével, M. Pellarin, M. Treilleux, J.L. Vialle, A. Perez, M. Broyer, Phys. Rev. Lett. 80 (1998) 5105.
[30] J. Sancho-Parramon, Nanotechnology 20 (2009) 235706.